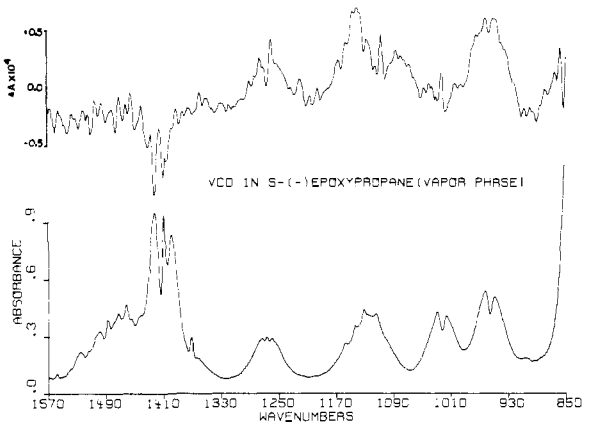

Figure 1. Vapor-phase vibrational circular dichroism in (*S*)-(−)-epoxypropane. The bottom trace is infrared absorption and the upper trace is VCD spectrum. VCD is obtained from 12 500 ac scans and 160 dc scans at 4-cm^{-1} resolution.

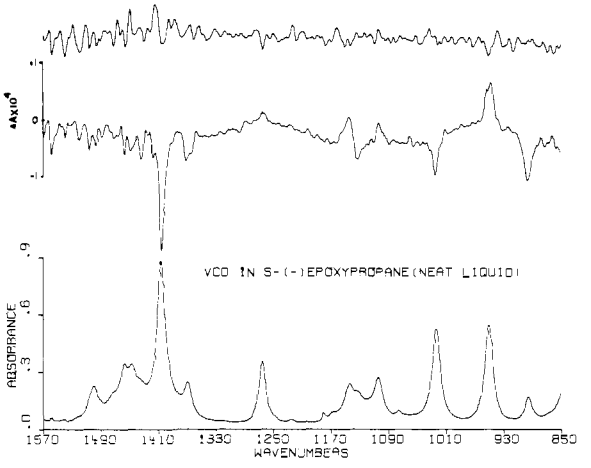

Figure 2. Liquid-phase vibrational circular dichroism in (*S*)-(−)-epoxypropane. The bottom trace is absorption spectrum and the middle trace is the VCD spectrum, which is obtained from 6250 ac scans and 80 dc scans at 4-cm^{-1} resolution. The top most spectrum is the difference between two such VCD measurements and represents the level of spectral reproducibility.

bands at 1023 and 950 cm^{-1} are associated with the degeneracy-lifted methyl rocking modes. The bands in vapor phase show splittings due to the resolution of rovibrational P, Q, and R band contours.

From the VCD spectra (Figures 1 and 2) it is noted that the symmetric methyl deformation mode exhibits negative VCD, but the degeneracy-lifted antisymmetric methyl deformation modes do not show any noticeable VCD features either in vapor or liquid phase. The degeneracy-lifted methyl rocking modes, however exhibit bisignate VCD both in vapor and liquid phases and support the theoretical concepts.[2,4] In vapor phase, the low-frequency component (at 950 cm^{-1}) exhibits sizeable positive VCD while the high-frequency component exhibits a small negative VCD. In liquid phase, VCD associated with both components is of nearly equal intensity. This difference in relative intensities is attributed to the Coriolis interactions[10] in vapor phase, because the absorption intensity perturbations at 1023 and 830 cm^{-1} in vapor phase point to the presence of such interactions.

Other differences apparent in vapor- and liquid-phase VCD spectra can be explained by broad rovibrational band contours in vapor phase. A striking difference in Figures 1 and 2 is noticed around 1130 cm^{-1} where a positive–negative–positive VCD triplet is present in liquid phase and a single positive VCD band is present in vapor phase. VCD bands are significantly broader in vapor phase due to the resolution of P, Q, and R band contours. As a consequence, VCD observed in vapor phase around 1130 cm^{-1} is actually the resulting sum of overlaping VCD contributed by P, Q, and R branches of three individual bands at 1143, 1130, and 1104 cm^{-1}. Similarly, the negative VCD at 1371 cm^{-1}, which is associated with the C*–H deformation mode, observed in liquid phase is submerged under VCD associated with the P branch of methyl symmetric deformation mode.

These observations suggest that, to explain vapor-phase VCD features quantitatively, the existing theoretical models need to be modified to incorporate Coriolis interactions and rovibrational transitions.

In the vapor-phase VCD spectrum, some fine structure corresponding to the P, Q, and R splittings of the absorption spectrum is evident. This fine structure gives the appearance of noise in both absorption and VCD spectrum. However, the noise level in vapor-phase spectrum is approximately the same as that in liquid phase, since in both spectra (see Figures 1 and 2) the overall absorption is nearly equal and the instrumental conditions are identical. The identification of fine structure is not essential for VCD intensities, because such fine structure should be broadened out by using pressure broadening techniques,[11] to obtain accurate intensity information.

Another significant observation in the present measurement is that the dissymmetry factor ($\Delta A/A$) is greater than 10^{-4} for most of the bands; for the molecules studied in the literature, the dissymmetry factors above 10^{-4} were less common. The maximum value noted here is 5×10^{-4}, for the band at 895 cm^{-1}, which is associated with the ring deformation and symmetric C–O stretch. This is one of the very few large values observed[12] thus far.

Acknowledgment. This work is supported by grants from NIH (GM29375) and Vanderbilt University. D.F.M. thanks Professor B. A. Hess, Jr., and the Department of Chemistry for a teaching appointment.

(10) Mills, I. M. *Pure Appl. Chem.* **1965**, *11*, 325.

(11) Wilson, E. B., Jr.; Wells, A. J. *J. Chem. Phys.* **1946**, *14*, 578. Penner, S. S.; Weber, D. *Ibid.* **1951**, *19*, 807.

(12) The largest dissymmetry factor (≃0.02) reported to date is for the azide band in azidomethemoglobin. See: Marcott, C.; Havel, H. A.; Hedlund, B.; Overend, J.; Moscowitz, A. In "Optical Activity and Chiral Discrimination"; Mason, S. F., Ed.; Reidel: Dordrecht, Holland, 1979.

^{19}F MAS-NMR of Fluoridated Hydroxyapatite Surfaces

James P. Yesinowski* and Michael J. Mobley

Miami Valley Laboratories
and Sharon Woods Technical Center
The Procter & Gamble Company, Cincinnati, Ohio 45247

Received December 2, 1982

High-resolution NMR of solids by magic-angle spinning (MAS) promises to be a useful spectroscopic technique for the characterization of solid surfaces.[1] We demonstrate here that high-field ^{19}F MAS-NMR can be used to provide new information about the fluoridation of hydroxyapatite surfaces. Calcium hydroxyapatite, $Ca_5(OH)(PO_4)_3$, is the prototypical mineral of bone and

(1) Stejskal, E. O.; Schaefer, J.; Henis, J. M. S.; Tripodi, M. K. *J. Chem. Phys.* **1974**, *61*, 2351–2355. Dawson, W. H.; Kaiser, S. W.; Ellis, P. D.; Inners, R. R. *J. Phys. Chem.* **1982**, *86*, 867–868. Chiang, C.-H.; Liu, N.-I.; Koenig, J. L. *J. Colloid Interface Sci.* **1982**, *86*, 26–34. Berni, L.; Clark, H. C.; Davies, J. A.; Drexler, D.; Fyfe, C. A.; Wasylishen, R. *J. Organomet. Chem.* **1982**, *224*, C5–C9. Maciel, G. E.; Sindorf, D. W. *J. Am. Chem. Soc.* **1980**, *102*, 7606–7607. Maciel, G. E.; Sindorf, D. W.; Seger, M. R.; Chuang, I.-S.; Shatlock, M. P. "Abstracts of Papers", 184th ACS National Meeting of the American Chemical Society, Kansas City, MO, Sept 1982; American Chemical Society: Washington, D.C., 1982; ANYL 16. Kotanigawa, T.; Shimokawa, K.; Yoshida, T. *J. Chem. Soc., Chem. Commun.* **1982**, 1185–1187. For a recent review of NMR of solids techniques with surface applications see: Duncan, T. M.; Dybowski, C. *Surf. Sci. Rep.* **1981**, *1*, 157–250.

0002-7863/83/1505-6191$01.50/0

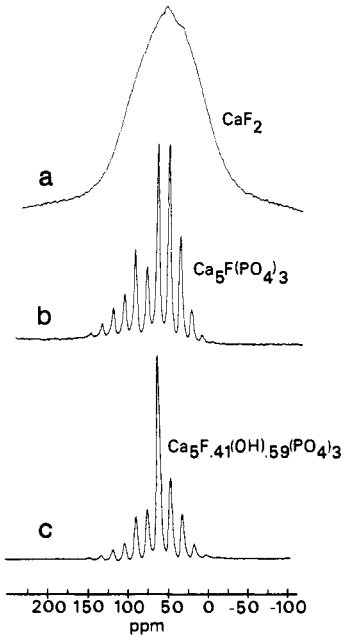

Figure 1. ^{19}F MAS-NMR spectra at 282.3 MHz of bulk reference compounds: (a) calcium fluoride (from MCB), spinning speed = 3.8 kHz, a 1-μs pulse ($\sim$15°) followed by a 7-μs delay before acquisition was used, and a line broadening of 282 Hz was applied; (b) synthetic fluoroapatite,[22] spinning speed = 3.80 kHz, 30° pulses, line broadening = 141 Hz, center peak at 64.0 ppm from C_6F_6 reference; (c) fluorohydroxyapatite with $x = 0.41$ (provided by Dr. E. C. Moreno[23]), spinning speed = 4.00 kHz, 30° pulses, line broadening = 141 Hz, center peak at 61.7 ppm from C_6F_6 reference.

tooth enamel. The hydroxyapatite surface has a remarkable avidity for fluoride, taking up this ion from aqueous solutions containing fluoride at the parts per million (50 μM) level.[2] XPS studies have shown that the fluoride is located on the surface.[3,4] An understanding of the details of this process is crucial to developing a complete explanation of the well-established anticaries effect of fluoride.[2] Possible modes of incorporation of fluoride include ion-exchange, adsorption, and crystal growth of calcium fluoride, fluoroapatite ($Ca_5F(PO_4)_3$), or fluorohydroxyapatite solid solutions ($Ca_5F_x(OH)_{1-x}(PO_4)_3$). Despite extensive efforts to distinguish these possible modes of fluoride incorporation by chemical,[5-7] spectroscopic,[3,4,8] and diffractometric[9,10] techniques, a reliable method for doing so has not yet been reported.

The surface-treated samples examined in this study were prepared using hydroxyapatite from Bio-Rad (Ca/P molar ratio = 1.65, specific surface area (BET) = 61.6 m^2/g). Ten milliliters of a concentrated hydroxyapatite slurry (0.1 g/mL) was added to 1 L of NaF treatment solution adjusted to pH 7.0 and having 25 mM NaCl as background electrolyte. After treatment for 1 h at 37 °C without stirring, the solid was filtered with a 0.22 μ Millipore filter and dried at 110 °C for 1 h. The amount of fluoride in the solid was determined by fluoride electrode measurements of the dissolved solids. The ^{19}F MAS-NMR spectra were obtained at 282.3 MHz on a Bruker CXP-300 spectrometer with a modified MAS probe[11] at comparable spinning speeds of about 3.8 kHz and with a spectral width of 100 kHz.

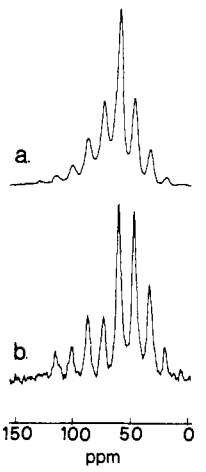

Figure 2. ^{19}F MAS-NMR spectra at 282.3 MHz of hydroxyapatite exposed to a (final) concentration of 9.7 mM (184 ppm) fluoride, total fluoride uptake = 0.68%: (a) several days after preparation, spinning rate = 3.86 kHz, 30° pulses at 1-s intervals, 300 scans, 80-Hz line broadening applied, real half-height line width = 5.9 ppm; (b) 6 months after preparation, spinning rate = 3.8 kHz, 30° pulses at 1-s intervals, 141-Hz line broadening applied, real half-height line width = 4.5 ppm.

For reference, ^{19}F MAS-NMR spectra of three *bulk-phase* fluoride compounds are shown in Figure 1. The spectra of fluoroapatite and the isomorphous fluorohydroxyapatite with $x = 0.41$ (Figure 1, b and c) are effectively narrowed by MAS at these moderate spinning speeds because of the inhomogeneous character of the broadening interactions.[11-16] The intensity pattern of the sidebands, which reflects these inhomogeneous interactions, varies with the degree of isomorphous substitution.[11] The spectrum of calcium fluoride, in contrast, is not significantly narrowed by MAS (Figure 1a) except at higher spinning speeds,[17] due to the homogeneous character of the broadening interactions.[12]

Figure 2a shows the ^{19}F MAS-NMR spectrum obtained several days after preparation of a sample of hydroxyapatite exposed to a (final) concentration of 9.7 mM F^-. A single peak 1.4 ppm upfield from that of fluoroapatite is observed, with associated sidebands. Both the slight upfield chemical shift and the increased relative intensity of the center peak correspond to a fluorohydroxyapatite spectrum with $0.4 < x < 0.8$ (cf. Figure 1c).[11] On the basis of the percentage of fluoride present and the specific surface area of the sample, there are 1.1 fluoride ions per surface hydroxyl site (assuming two hydroxyl sites per 65 $Å^2$, the area of an *ac* or *bc* face[16]). The NMR spectrum is thus consistent with the presence of a surface layer of fluorohydroxyapatite. The ^{19}F MAS-NMR spectrum of the same powdered sample after 6 months[18] (Figure 2b) is characteristic of fluoroapatite and did not change further after an additional 4 months. Thus, ^{19}F MAS-NMR reveals a gradual change in the environment of the fluoride ion from hydroxyl group neighbor(s) to (two) fluoride neighbors along the *c* axis.[16] This solid-state transformation is

(2) Brown, W. E.; Konig, K. G., Eds. *Caries Res.* **1977**, *11*, Suppl. 1, 1–327.
(3) Hercules, D. M.; Craig, N. L. *J. Dent. Res.* **1976**, *55*, 829–835.
(4) Lin, J.; Raghavan, S.; Fuerstenau, D. W. *Colloids Surf.* **1981**, *3*, 357–370.
(5) McCann, H. G. *J. Biol. Chem.* **1953**, *201*, 247–259.
(6) Spinelli, M. A.; Brudevold, F.; Moreno, E. *Arch. Oral Biol.* **1971**, *16*, 187–203.
(7) Caslavska, V.; Moreno, E. C.; Brudevold, F. *Arch. Oral Biol.* **1975**, *20*, 333–339.
(8) Menzel, B.; Amberg, C. H. *J. Colloid Interface Sci.* **1972**, *38*, 256–264.
(9) Francis, M. D.; Gray, J. A.; Griebstein, W. J. *Adv. Oral Biol.* **1968**, *3*, 83–120.
(10) Baud, C. A.; Bang, S. *Caries Res.* **1970**, *4*, 1–13.
(11) Yesinowski, J. P.; Wolfgang, R. A.; Mobley, M. J., poster and abstract, 23rd Experimental NMR Conference, Madison, WI, 1982. Yesinowski, J. P.; Wolfgang, R. A.; Mobley, M. J. In "Adsorption on and Surface Chemistry of Hydroxyapatite"; Misra, D. N., Ed.; Plenum Press: New York, in press.
(12) Maricq, M. M.; Waugh, J. S. *J. Chem. Phys.* **1979**, *70*, 3300–3316.
(13) Carolan, J. L. *Chem. Phys. Lett.* **1971**, *12*, 389–391.
(14) Knoubovets, R. G.; Afanasjev, M. L.; Habuda, S. P. *Spectrosc. Lett.* **1969**, *2*, 121–125.
(15) Vakhrameev, A. M.; Gabuda, S. P.; Knoubovets, R. G. *J. Struct. Chem. (Engl. Transl.)* **1978**, *19*, 256–261.
(16) Kay, M. I.; Young, R. A.; Posner, A. S. *Nature (London)* **1964**, *204*, 1050–1052.
(17) Lowe, I. J. *Phys. Rev. Lett.* **1959**, *2*, 285–287.
(18) Stored in a screw-capped rotor at ambient temperature and humidity.
(19) Other samples we have investigated show that during the first month after preparation the ^{19}F MAS-NMR spectra gradually sharpen but still resemble fluorohydroxyapatite spectra; after 3 months the spectra resemble the fluoroapatite spectrum (e.g., Figure 3b).

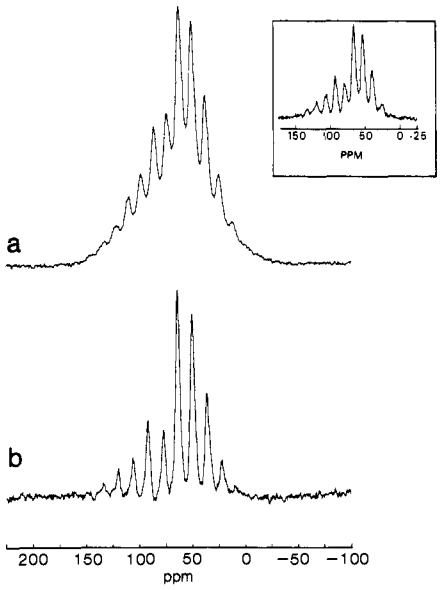

Figure 3. ^{19}F MAS-NMR spectra at 282.3 MHz of hydroxyapatite exposed to fluoride, aged 14 (a) and 10 (b) months after preparation: (a) 155.3 mM (2950 ppm) final fluoride concentration, total fluoride uptake = 2.2%, spinning rate = 3.80 kHz, 45° pulses at 1-s intervals; Insert shows spectrum of same sample obtained using Hahn spin–echo (90_x–263 μs–180_y–263 μs–acquire), 90° pulse = 3.2 μs; the delay time must be set to an integral multiple of the sample rotation period to obtain a good spectrum.[24] (b) 9.7 mM (184 ppm) final fluoride concentration, total fluoride uptake = 0.68%, spinning rate = 3.84 kHz, 45° pulses at 1-s intervals. Center peak of fluoroapatite component in both samples is at 63.3 ppm.

probably due to diffusion of the ions over the surface of the crystallites, rather than to any bulk-phase transformation.

The effect of the aqueous fluoride concentration on samples aged for many months after isolation is shown in Figure 3, a and b. The ^{19}F MAS-NMR spectrum of the lower concentration sample (Figure 3b) shows the presence of only fluoroapatite (cf. Figure 1b). In marked contrast, the sample exposed to the higher fluoride concentration exhibits sharp peaks characteristic of apatitic fluoride superimposed upon a broad peak (Figure 3a). We assign the broad component to calcium fluoride on the basis of its chemical shift position and large line width. Furthermore, calcium fluoride is the only non-apatitic form of fluoride that is known to form at higher fluoride concentrations.[2,4,5,9]

Identification and quantitation of the apatitic component in a spectrum such as that in Figure 3a is hindered by the substantial broad peak arising from calcium fluoride. It is possible to eliminate the calcium fluoride signal from the spectrum by taking advantage of the fact that the spin–spin relaxation time T_2 of calcium fluoride is 2 orders of magnitude smaller than that of fluoroapatite.[11] The insert in Figure 3a shows a ^{19}F MAS-NMR spectrum of the same sample obtained by using a Hahn spin–echo pulse sequence.[20] All of the signal from calcium fluoride has decayed, leaving only the signal from the apatitic component, whose chemical shift and sideband intensities are indicative of fluoroapatite. The use of the Hahn spin–echo enables one to obtain good spectra of the apatitic component alone in these surface samples, and should make possible more accurate quantitation of the relative amounts of calcium fluoride and fluoroapatite. These data provide spectroscopic evidence for the onset of calcium fluoride formation at high concentrations[2,4,5,9] and reveal as well that fluoroapatite coexists with the calcium fluoride. It is significant that an apatitic form of fluoride has been detected in all of the numerous samples we have investigated. This observation suggests that the surface fluoride ion occupies its normal position in the apatitic lattice[16] and is surrounded by a triangle of three calcium atoms as in the bulk solid. No evidence for a second site of incorporation has been seen.

In summary, high-field ^{19}F MAS-NMR is a powerful method for investigating the fluoridated surface of hydroxyapatite. It selectively probes *only* the fluoride environment and quantitatively detects *all* the fluoride present, whether crystalline, amorphous, or adsorbed.[21] The spectral appearance is very sensitive to the form of fluoride, and many NMR parameters can be used to characterize the samples. Low levels of fluoride (<0.1%) can be detected, making possible the study of biological calcified tissue. Applications to the study of fluoride in other minerals, either on surfaces or in the bulk, should also prove very fruitful.

Acknowledgment. We thank Rex Wolfgang and Robert Faller for invaluable technical assistance.

(20) Abragam, A. "The Principles of Nuclear Magnetism"; Oxford University Press: London, 1971; pp 33–34, 58–63.

(21) Integration of the fluoride signal obtained under nonsaturating conditions yields fluoride concentrations in agreement with those determined from chemical analysis.

(22) McCann, H. G. *Arch. Oral Biol.* **1968**, *13*, 987–1001.
(23) Moreno, E. C.; Kresak, M.; Zahradnik, R. T. *Caries Res.* **1977**, *11*, Suppl. 1, 142–171.
(24) Dixon, W. T. *J. Chem. Phys.* **1982**, *77*, 1800–1809.

Thioether Trans-Cross-Linking Reaction of Phalloidin[1]

Theodor Wieland,* Michael Nassal, Tamiko Miura,[2] and Christa Götzendörfer

Max-Planck-Institut für Medizinische Forschung
6900 Heidelberg, West Germany
Received May 13, 1983

Phalloidin (**1a**), one of the toxic components of the poisonous

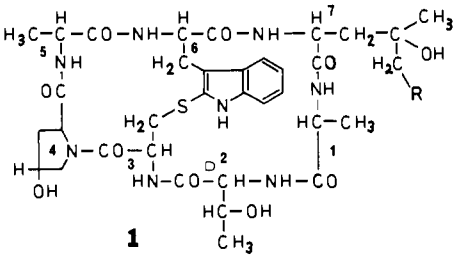

1

1a, R = OH
1b, R = OTos

fungus *Amanita phalloides*,[3] is a *bicyclic* heptapeptide cross-linked by a sulfur atom between the 2-position of the indole ring of a tryptophan and the methylene of a cysteine residue.[4] Its positive helicity of the (inherently) unsymmetric thioether chromophore gives rise to the positive Cotton effects (around 240 and 300 nm, Figure 1) in the CD spectrum.[5]

The likewise toxic virotoxins from *Amanita virosa* are *monocyclic* heptapeptides containing a methylsulfonyl group instead of the thioether cross-link.[6] Attempts were made to transform **1a** to viroidin by cleaving this bridge. However, methylation of the sulfur and β-elimination of the desired methylsulfonium ion failed. Hence, it was intriguing to find an intramolecular alkylation of the thioehter as the first step of a trans cross-linking in the bicyclic system.

(1) Dedicated to Dr. Ulrich Weiss, National Institutes of Health, Bethesda, MD, on the occasion of his 75th birthday.
(2) Miura, Tamiko, visiting student, 1980–1981. Present address: Science University of Tokyo, Department of Chemistry, Kagurazaka, Shinyuku-ku Tokyo, Japan.

(3) Lynen, F.; Wieland, U. *Liebigs Ann. Chem.* **1938**, *533*, 93–117.
(4) Wieland, Th.; Schön, W. *Liebigs Ann. Chem.* **1955**, *593*, 157–178. Wieland, Th.; Schnabel, H. W. *Liebigs Ann. Chem.* **1962**, *657*, 225–228.
(5) Wieland, Th.; Beijer, B.; Seeliger, A.; Dabrowski, J.; Zanotti, G.; Tonelli;, A. E.; Gieren, A.; Dederer, B.; Lamm, V.; Hädicke, E. *Liebigs Ann. Chem.* **1981**, 2318–2334.
(6) Faulstich, H.; Buku, A.; Bodenmüller, H.; Wieland, Th. *Biochemistry* **1980**, *19*, 3334–3343.

0002-7863/83/1505-6193$01.50/0